A SIMPLE NONLOCAL DAMAGE MODEL FOR PREDICTING FAILURE OF NOTCHED LAMINATES

by

T.C. Kennedy and M.F. Nahan

Department of Mechanical Engineering
Oregon State University
Corvallis, OR 97331

Accepted for publication in *Composite Structures*

ABSTRACT

The ability to predict failure loads in notched composite laminates is a requirement in a variety of structural design circumstances. A complicating factor is the development of a zone of damaged material around the notch tip. The objective of this study was to develop a computational technique that simulates progressive damage growth around a notch in a manner that allows the prediction of failure over a wide range of notch sizes. This was accomplished through the use of a relatively simple, nonlocal damage model that incorporates strain-softening. This model was implemented in a two-dimensional finite element program. Calculations were performed for two different laminates with various notch sizes under tensile loading, and the calculations were found to correlate well with experimental results.

1 INTRODUCTION

The design of structural components made of composite materials is heavily influenced by damage tolerance requirements. The problem of predicting failure in notched laminates has been the subject of numerous studies. A review of those occurring before 1985 can be found in Awerbuch and Madhukar.[1] All failure theories that have been developed contain empirical parameters such as a characteristic length. Unfortunately, these parameters are not always true material properties because they appear to be functions of notch size; i.e., the parameter value that leads to a correct failure prediction for small notches does not usually work well with large notches.[2]

In a composite material a zone of damage of considerable influence is known to develop in advance of a crack. Recent research[3] indicates that the damage growth in the vicinity of the crack tip manifests itself in the form of strain-softening of the material. Strain-softening models have received a great deal of attention for describing the fracture of concrete and other materials where microstructure has a strong influence on macroscopic properties. In general, a macroscopic description of damage (e.g., distributed cracking) is reflected in a constitutive model that exhibits a decrease of stress with increasing strain beyond some critical strain ϵ_d as shown in Fig. 1. The incorporation of strain-softening into a finite element analysis based on classical plasticity theory results in calculations that are mesh sensitive. This occurs because as the mesh is refined, there is a tendency for the damage zone to localize to a zero volume. This leads to the prediction of structural failure with zero energy dissipation, which is physically impossible. Numerous techniques have been proposed to address this issue.

Two of these techniques that hold promise for modeling damage growth in composite structures are the discrete crack model and the nonlocal damage model. The discrete crack model avoids the zero energy dissipation problem by using a stress-displacement law over the damage

zone rather than a stress-strain law. These models were pioneered by Hillerborg et al.[4] who used a Dugdale-Barrenblat[5,6] type model to represent the damage zone ahead of the crack. Backlund and Aronsson[7,8] extended this concept to composite materials. This approach is straightforward but lacks generality because the crack path must be assumed beforehand. Alternatively, the nonlocal damage model offers the same advantages of the discrete crack model but avoids its shortcomings.

Rudimentary damage mechanics based upon local constitutive relations can be used to successfully model strain softening. Better yet, damage evolution based upon the concept of a nonlocal continuum prevents unacceptable localization of the damage. The basic idea in a nonlocal continuum is that the stress at a point in a body is dependent on the strains of neighboring points in addition to the strain at the point. In its most general form, this theory, which can be tied to a statistical analysis of heterogeneous materials, can lead to nearly intractable mathematical complexity. Bazant and Chang[9] modified this theory and incorporated it into a finite element analysis that could handle strain-softening without spurious mesh sensitivity. Unfortunately, this approach proved to be inconvenient in practical applications because it required an imbricated system of elements overlapping one another. Recently, Bazant and Pijaudier-Cabot[10] removed this difficulty with the introduction of a nonlocal damage theory which incorporates nonlocal principles into continuum damage mechanics. In this theory only the damage parameter is considered to be nonlocal (i.e., a function of the strain averaged from a certain neighborhood of a point) while all other variables are local. Bazant[11] justified the validity of this approach using a simplified micromechanical analysis to show that fracturing strain due to damage is the result of the release of stored energy from a finite size microcrack neighborhood. Bazant and Lin[12] incorporated the nonlocal damage concept into a two-dimensional finite element analysis and

applied it successfully in predicting failure of concrete. DeVree et al.[13] also developed a nonlocal damage finite element analysis for isotropic materials.

The objective of this study was to develop a technique that simulates progressive damage growth around a notch in a composite laminate and that can be used to predict failure. This was accomplished by applying a relatively simple nonlocal damage model to fiber-reinforced composites. This model was implemented in a two-dimensional finite element program. Calculations were performed, and the results were compared to data from fracture tests.

2 STRESS-STRAIN RELATIONS FOR A DAMAGED LAMINATE

The analysis of a composite laminate will not be done on a ply-by-ply basis, but rather it will simply be considered as a homogeneous material with orthotropic material properties. Treating the material as being in a state of plane stress, the stress-strain relations in principal material coordinates (x_1 and x_2) for undamaged material can be written as

$$\{\epsilon\} = [C]^{-1}\{\sigma\} \tag{1}$$

where

$$\{\epsilon\}^T = [\epsilon_1 \;\; \epsilon_2 \;\; \gamma_{12}] \tag{2}$$

$$\{\sigma\}^T = [\sigma_1 \;\; \sigma_2 \;\; \tau_{12}] \tag{3}$$

$$C_{11} = E_1/(1 - \nu_{12}\,\nu_{21}) \,,\; C_{22} = E_2/(1 - \nu_{12}\,\nu_{21}) \,,\; C_{33} = G_{12}$$

$$C_{12} = C_{21} = \nu_{12}\,E_2/(1 - \nu_{12}\,\nu_{21}) \,,\; C_{13} = C_{23} = C_{31} = C_{32} = 0 \,. \tag{4}$$

When damage occurs (microcracking, etc.) the effective load-carrying area of the material is reduced. We introduce the concept of an effective stress[14] $\tilde{\sigma} = \sigma/(1\text{-}D)$ to account for this area reduction. The quantity D is the damage variable which ranges from 0 (no damage) to 1 (development of a macrocrack). For simplicity we assume that damage develops independently in

the x_1 and x_2 directions. For this orthotropic damage development, the effective stress can be expressed in general form as[15]

$$\{\tilde{\sigma}\} = [M]\,\{\sigma\} \tag{5}$$

where

$$\{\tilde{\sigma}\}^T = [\tilde{\sigma}_1 \;\; \tilde{\sigma}_2 \;\; \tilde{\tau}_{12}] \tag{6}$$

$$M_{11} = 1/(1-D_1)\;,\; M_{22} = 1/(1-D_2)\;,\; M_{33} = 1/\sqrt{1-D_1}\,\sqrt{1-D_2}$$
$$M_{12} = M_{13} = M_{23} = M_{21} = M_{31} = M_{32} = 0\;. \tag{7}$$

We now take the same approach as Chow and Wang[15] and use the elastic energy equivalence concept that states that the complementary elastic energy for a damaged material is in the same form as that of an undamaged material except that the stress is replaced by the effective stress in the energy formulation, i.e.,

$$\mathbb{W} = \frac{1}{2}\,\{\sigma\}^T\,[C]^{-1}\,\{\sigma\} \tag{8}$$

$$= \frac{1}{2}\,\{\sigma\}^T\,[M]^T\,[C]^{-1}\,[M]\,\{\sigma\}\;. \tag{9}$$

The stress-strain equation for a damaged material can be written as

$$\{\epsilon\} = \frac{\partial \mathbb{W}}{\partial\{\sigma\}} = [M]^T\,[C]^{-1}\,[M]\,\{\sigma\} \tag{10}$$

or

$$\{\epsilon\} = [\tilde{C}]^{-1}\,\{\sigma\} \tag{11}$$

where

$$[\tilde{C}]^{-1} = [M]^T\,[C]^{-1}\,[M] \tag{12}$$

Alternatively, we can write

$$\{\sigma\} = [\tilde{C}]\ \{\epsilon\} \tag{13}$$

where

$$\begin{aligned}
\tilde{C}_{11} &= E_1\ (1-D_1)^2\ /\ (1-\nu_{12}\nu_{21}) \\
\tilde{C}_{12} &= \tilde{C}_{21} = \nu_{21}E_1\ (1-D_1)\ (1-D_2)\ /\ (1-\nu_{12}\nu_{21}) \\
\tilde{C}_{22} &= E_2\ (1-D_2)^2\ /\ (1-\nu_{12}\nu_{21}) \\
\tilde{C}_{33} &= G_{12}\ (1-D_1)\ (1-D_2) \\
\tilde{C}_{13} &= \tilde{C}_{23} = \tilde{C}_{31} = \tilde{C}_{32} = 0\ .
\end{aligned} \tag{14}$$

In the finite element formulation, we may have the material coordinates x_1 and x_2 at some angle θ relative to the global coordinates x and y. We can transform the stresses and strains through the usual transformation relations to get

$$\{\sigma\} = [T_\sigma]\ \{\sigma'\} \tag{15}$$

and

$$\{\epsilon\} = [T_\epsilon]\ \{\epsilon'\} \tag{16}$$

where

$$\{\sigma'\}^T = [\sigma_x\ \ \sigma_y\ \ \tau_{xy}] \tag{17}$$

$$\{\epsilon'\}^T = [\epsilon_x\ \ \epsilon_y\ \ \gamma_{xy}] \tag{18}$$

$$[T_\sigma] = \begin{bmatrix} \cos^2\theta & \sin^2\theta & 2\sin\theta\cos\theta \\ \sin^2\theta & \cos^2\theta & -2\sin\theta\cos\theta \\ -\sin\theta\cos\theta & \sin\theta\cos\theta & \cos^2\theta - \sin^2\theta \end{bmatrix} \tag{19}$$

$$[T_\epsilon] = \begin{bmatrix} \cos^2\theta & \sin^2\theta & \sin\theta\cos\theta \\ \sin^2\theta & \cos^2\theta & -\sin\theta\cos\theta \\ -2\sin\theta\cos\theta & 2\sin\theta\cos\theta & \cos^2 -\sin^2\theta \end{bmatrix}. \tag{20}$$

Combining eqns (13), (15), and (16) gives

$$\{\sigma'\} = [\tilde{C}'] \{\epsilon'\} \tag{21}$$

where

$$[\tilde{C}'] = [T_\sigma]^{-1} [\tilde{C}] [T_\epsilon] . \tag{22}$$

3 DAMAGE DEVELOPMENT

In the nonlocal damage model, the damage parameters D_1 and D_2 are assumed to be functions of the nonlocal strains $\bar{\epsilon}_1$ and $\bar{\epsilon}_2$ defined as

$$\bar{\epsilon}_1(x,y) = \frac{1}{A_r(x,y)} \iint_A \alpha(\xi-x, \eta-y)\, \epsilon_1(\xi,\eta)\, d\xi\, d\eta \tag{23}$$

$$\bar{\epsilon}_2(x,y) = \frac{1}{A_r(x,y)} \iint_A \alpha(\xi-x, \eta-y)\, \epsilon_2(\xi,\eta)\, d\xi\, d\eta \tag{24}$$

where

$$A_r(x,y) = \iint_A \alpha(\xi-x, \eta-y)\, d\xi\, d\eta \tag{25}$$

and $\alpha(\xi\text{-}x, \eta\text{-}y)$ is a weight function which we have chosen in the form suggested by Bazant,[16] i.e.,

$$\alpha(\xi-x, \eta-y) = \left\{1 - \left[\frac{(\xi-x)^2 + (\eta-y)^2}{0.8256\, \ell^2}\right]\right\}^2 \tag{26}$$

where ℓ is the characteristic length for the material, and α equals zero if the quantity within brackets becomes negative. The relationship between the damage parameter and the nonlocal strain is determined from the stress-strain curve. Consider the case of a uniaxial load σ_o in the x_1 direction. For this case eqn (11) gives

$$\epsilon_1 = \sigma_o / E_1(1 - D_1)^2 . \tag{27}$$

Since ϵ_1 is uniform, the nonlocal strain $\bar{\epsilon}_1$ is simply equal to ϵ_1 for all points except those in a boundary layer around the edges which will be ignored. Solving eqn (27) for D_1 gives

$$D_1 = 1 - (\sigma_o / E_1 \bar{\epsilon}_1)^{1/2} . \tag{28}$$

The shape of the stress-strain curve after the initiation of damage (i.e., the relationship between σ_1 and ϵ_1 for $\epsilon_1 > \epsilon_{1d}$) determines how D_1 is related to $\bar{\epsilon}_1$. This ultimately leads to an explicit mathematical representation for D_1 as

$$D_1 = f_1 (\bar{\epsilon}_1) . \tag{29}$$

A similar relationship can be found for D_2, i.e.,

$$D_2 = f_2 (\bar{\epsilon}_2) . \tag{30}$$

Equations (21), (23), (24), (29), and (30) completely describe the stress-strain behavior of the laminate.

4 FINITE ELEMENT FORMULATION

To develop a finite element formulation for progressive damage analysis, we begin with the principle of virtual work[17]

$$\int_V \{\hat{\epsilon}'\}^T \{\sigma'\} \, dV = \int_S \{\hat{u}\}_S^T \{f\} \, ds \tag{31}$$

where $\{\hat{\epsilon}'\}$ is the strain associated with the virtual displacement $\{\hat{u}\}$, $\{\hat{u}\}_S$ is the virtual displacement of the surface of the body, and $\{f\}$ is the traction on the surface of the body. We will develop this analysis for an 8-node quadrilateral element. Using the usual shape functions of this element,[18] we can express the displacement $[u]_m$ within an element m in terms of the nodal displacement $\{U\}$ as

$$\{u\}_m = [L]_m \{U\} . \tag{32}$$

Applying the two-dimensional strain-displacement relations to eqn (32), we arrive at the following relation[18] between strain and nodal displacement

$$\{\epsilon'\}_m = [B]_m \{U\} . \tag{33}$$

Substituting eqns (32) and (33) into eqn (31) gives

$$\sum_m \int_{V_m} [B]_m^T \{\sigma'\}_m \, dV_m = \sum_m \int_{S_m} [L]_{S_m}^T \{f\}_m \, dS_m . \tag{34}$$

Substituting eqn (21) into eqn (34) gives

$$\left(\sum_m \int_{V_m} [B]_m^T [\tilde{C}']_m [B]_m \, dV_m \right) \{U\} = \sum_m \int_{S_m} [L]_{S_m}^T \{f\}_m \, dS_m . \tag{35}$$

We now set

$$[K] = \sum_m \int_{V_m} [B]_m^T [\tilde{C}']_m [B]_m \, dV_m , \tag{36}$$

$$\{R\} = \sum_m \int_{S_m} [L]_{S_m}^T \{f\}_m \, dS_m . \tag{37}$$

Thus

$$[K] \{U\} = \{R\} \tag{38}$$

where [K] is the stiffness matrix and {R} is the generalized nodal load matrix. After damage initiates, eqn (38) represents a nonlinear system of algebraic equations because [K] is a function of D_1 and D_2 which depend on the nonlocal strains. The nonlocal strains in eqns (23) and (24) are evaluated numerically using Gaussian integration. Equation (38) can be solved iteratively using the Newton-Raphson method.[17]

Based on the above analysis, a computer program was developed and calculations were performed for the case of a center-cracked plate under tension, as shown in Fig. 2. It was found that convergence difficulties arose for materials whose stress-strain curves had softening regimes with steep slopes. To overcome these difficulties we made use of a procedure based on the concept of viscous relaxation.[19] We introduced a small amount of viscous damping into the

analysis and treated the problem dynamically (without inertia effects) so that eqn (38) was replaced by

$$[C_d]\{\dot{U}\} + [K]\{U\} = \{R\} \tag{39}$$

where $[C_d]$ is the damping matrix and $\{\dot{U}\}$ is the time derivative of $\{U\}$. To solve the above differential equations numerically, we used the trapezoidal rule of time integration,[17] i.e.,

$$^{t+\Delta t}\{U\} = {}^{t}\{U\} + \Delta t\,(\,{}^{t}\{\dot{U}\} + {}^{t+\Delta t}\{\dot{U}\})/2 \tag{40}$$

where the superscript in front of the variable indicates the time at which it is evaluated. For the damping matrix we employed Rayleigh damping, i.e.,

$$[C_d] = \beta\,[K]\,. \tag{41}$$

We found that a value of $\beta = 0.01$ sec^{-1} for a time step $\Delta t = 1$ sec eliminated the convergence problems and also reproduced results that were within a fraction of a percent of previous static calculations.

5 RESULTS

Calculations were performed for a 13-ply laminate of graphite/epoxy with a [45/-45/90/0/60/-60/90/-60/60/0/90/-45/45] lay-up. The laminate stiffness properties were E_x =36.3 GPa, E_y =61.5 GPa, $\nu_{xy} = 0.28$, and G_{xy} =20.7 Gpa.. The softening portions of the stress-strain curves were represented by exponential functions:

$$\sigma_x = E_x \epsilon_{dx} e^{-a_x(\epsilon_x - \epsilon_{dx})} \tag{42}$$

$$\sigma_y = E_y \epsilon_{dy} e^{-a_y(\epsilon_y - \epsilon_{dy})} \tag{43}$$

with $\epsilon_{dx} = 0.01101$, $a_x = 2000$, $\epsilon_{dy} = 0.00984$, $a_y = 600$, and a characteristic length $\ell = 0.762$ cm. The stress-strain curve for the y-direction is shown in Fig. 1. The values for ϵ_{dx} and ϵ_{dy} came from tensile tests.[2] Measuring the softening properties in a standard tensile test is extremely

difficult to do.[20] Therefore, these values were chosen in an inverse manner to match data from fracture tests described next.

A center-cracked plate under tension as shown in Fig. 2 was analyzed with the program for a crack length 2a = 6.35 cm. and a specimen width W = 25.4 cm. An applied load σ_o was simulated by gradually displacing the top boundary while holding the bottom boundary fixed as would be done in a tensile test. Load versus displacement was monitored during the calculation, and when the load reached its peak value and began to decline, the specimen was assumed to fail. Calculations were performed for three different quarter-symmetry meshes as shown in Fig. 3 where MESH 1 is a coarse mesh, MESH 2 is a moderately fine mesh, and MESH 3 is a very fine mesh. A reflecting algorithm had to be used to correctly calculate nonlocal strains in elements near a symmetry boundary. The load versus displacement results for these three meshes are shown in Fig. 4. It can be seen that the solution converges with mesh refinement, and the difference in failure load between MESH 2 and MESH 3 is less than 0.5 percent. The calculations were repeated for various crack lengths between 0 and 30.5 cm. with W/2a = 4. A plot of nominal failure stress (applied force divided by total cross-sectional area) versus crack length is shown in Fig. 5. Also shown are experimental results from fracture tests.[2] It can be seen that the theory is capable of representing the failure load over a wide range of crack lengths.

The extent of the damage zone (i.e., material that has passed into the strain-softening regime) was also monitored during the calculation. As expected, the damage zone originated near the crack tip and grew primarily in the horizontal direction away from the tip. The distance from the crack tip to the outer edge of the damage zone as a function of load for three different crack lengths is shown in Fig. 6. In each case damage does not initiate until the applied load is very close to the failure load. After damage initiates, it grows rapidly.

The calculations just described were repeated for a 15-ply laminate of graphite/epoxy with a [-45/45/0/90/-30/30/-75/0/75/30/-30/90/0/45/-45] lay-up. The laminate stiffness properties were E_x=56.0 Gpa, E_y=46.5 Gpa, ν_{xy}=0.342, and G_{xy}=19.6 Gpa. Again, the softening portions of the stress-strain curves were represented by exponential functions with ϵ_{dx}=0.0072, a_x=20, ϵ_{dy}=0.0072, a_y=20, and a characteristic length ℓ=0.254 cm. The stress-strain curve for the y-direction for this laminate is shown in Fig. 7. Comparing this to Fig. 1, we observe that the softening portion of the curve for this laminate is much less steep than that of the 13-ply laminate.

A plot of nominal failure stress versus crack length for the 15-ply laminate is shown in Fig. 8 along with the corresponding experimental results. Again, the theory has performed well in representing the failure load over a wide range of crack lengths. The distance to the outer edge of the damage zone as a function of load for three crack lengths is shown in Fig. 9. Comparing this to the results in Fig. 6, we observe that the growth of the damage zone with applied load for this laminate is considerably more gradual than that for the 13-ply laminate. Overall, the 15-ply laminate exhibits less brittle behavior than does the 13-ply laminate as one would expect from the softening portion of their stress-strain curves.

6 CONCLUSION

In this study a progressive damage model for predicting failure loads in notched composite laminates was developed. This was based on relatively simple, nonlocal damage mechanics incorporating strain-softening. A two-dimensional finite element program was developed, and calculations were performed for two different laminates under tensile loading. One laminate exhibited "brittle" strain-softening response, and the other exhibited "ductile" strain-softening response. The theory was shown to accurately predict failure of these laminates over a wide

range of notch sizes. This approach clearly shows promise as a design tool for assessing damage tolerance because it has the potential for studying the response of a structure after a crack has begun to propagate. However, a number of issues need further study. These include the choice of mathematical function used to represent the strain-softening portion of the stress-strain curve and the effect of flexure. These topics will be addressed in future research.

Acknowledgment - This work was supported by NASA grant NAG-1-1620 monitored by J. H. Starnes. The authors wish to acknowledge helpful discussions with L. B. Ilcewicz, T. H. Walker, and D. P. Dopker of Boeing Commercial Airplane Company during the course of this research.

REFERENCES

1. Awerbuch, J. & Madhukar, M.S., Notched strength of composite laminates: predictions and experiments – a review. *Journal of Reinforced Plastics and Composites*, **4** (1) (1985) 1-159.

2. Walker, T.H., Ilcewicz, L.B., Polland, D.R. & Poe, C.C., Tension fracture of laminates for transport fuselage – part 2: large notches. *Third NASA Advanced Technology Conference*, NASA CP 3178, (1992) 727-758.

3. Ilcewicz, L.B., Walker, T.H., Murphy, D.P., Dopker, B. & Scholz, D.B., Tension fracture of laminates for transport fuselage – part 4: damage tolerance analysis. *Fourth NASA Advanced Technology Conference*, NASA CP 3229, (1993) 264-298.

4. Hillerborg, A., Modeer, M. & Petersson, P.E., Analysis of crack formation and crack growth in concrete by means of fracture mechanics and finite elements. *Cement Concrete Research*, **6** (1976) 773-782.

5. Dugdale, D.S., Yielding of steel sheets containing slits. *Journal of the Mechanics and Physics of Solids*, **8** (1960) 100-104.

6. Barenblatt, G.I., The mathematical theory of equilibrium cracks in brittle fracture. *Advances in Applied Mechanics*, **7** (1962) 55-129.

7. Backlund, J. & Aronsson, C.G., Tensile fracture of laminates with holes. *Journal of Composite Materials*, **20** (5) (1986) 259-286.

8. Aronsson, C.G. & Backlund, J., Tensile fracture of laminates with cracks. *Journal of Composite Materials*, **20** (5) (1986) 287-307.

9. Bazant, Z.P. & Chang, T.P. Nonlocal finite element analysis of strain softening solids. *Journal of Engineering Mechanics*, **113** (1987) 89-105.

10. Pijaudier-Cabot, G. & Bazant, Z.P., Nonlocal damage theory. *Journal of Engineering Mechanics*, **113** (1987) 1512-1533.

11. Bazant, Z.P., Why continuum damage is nonlocal: justification by quasiperiodic micro-crack array. *Mechanics Research Communications*, **14** (1987) 407-419.

12. Bazant, Z.P. & Lin, F.B., Nonlocal smeared crack model for concrete fracture. *Journal of Structural Engineering*, **114** (1988) 2493-2510.

13. De Vree, J.H.P, Brekelmans, W.AM. & Gils, M.A.J., Comparison of nonlocal approaches in continuum damage mechanics. *Computers & Structures*, **55** (4) (1995) 581-588.

14. Lemaitre, J., *A Course on Damage Mechanics*, Springer-Verlag, New York, 1992.

15. Chow, C.L. & Wang, J., An anisotropic theory of elasticity for continuum damage mechanics. *International Journal of Fracture*, **33** (1987) 3-16.

16. Bazant, Z.P. & Cedolin, L., *Stability of Structures: Elastic, Inelastic, Fracture, and Damage Theories*, Oxford University Press, New York, 1991.

17. Bathe, K.J., *Finite Element Procedures in Engineering Analysis*, Prentice-Hall, Englewood Cliffs, New Jersey, 1982.

18. Hinton, E. & Owen, D.R.J., *Finite Element Programming*, Academic Press, New York, 1977.

19. Webster, R.L., On the static analysis of structures with strong geometric nonlinearity. *Computers & Structures*, **11** (1980) 137-145.

20. Bazant, Z.P. & Pyandier-Cabot, G., Measurement of characteristic length of nonlocal continuum. *Journal of Engineering Mechanics*, **115** (1989) 755-767.

List of Figures

Fig. 1. Stress-strain curve for a laminate with strain-softening.

Fig. 2. Center-cracked tension specimen.

Fig. 3. Quarter-symmetry finite element meshes for a center-cracked tension specimen.

Fig. 4. Load-displacement curves for a center-cracked tension specimen modeled with three different finite element meshes.

Fig. 5. Nominal failure stress versus crack length for a center-cracked tension specimen (13-ply laminate).

Fig. 6. Applied load versus damage zone distance for three different crack lengths (13-ply laminate).

Fig. 7. Stress-strain curve for the 15-ply laminate.

Fig. 8. Nominal failure stress versus crack length for a center-cracked tension specimen (15-ply laminate).

Fig. 9. Applied load versus damage zone distance for three different crack lengths (15-ply laminate).

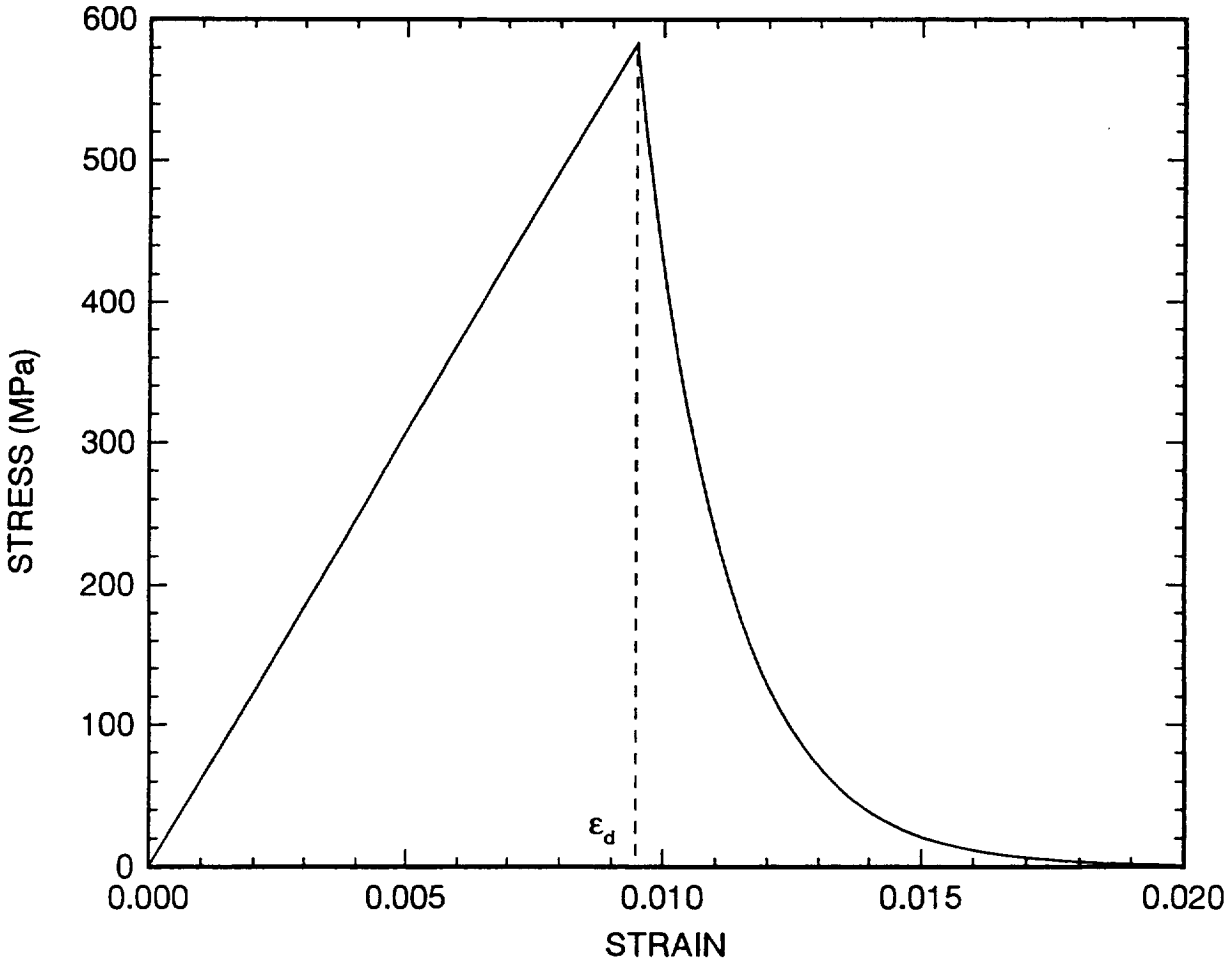

Fig. 1. Stress-strain curve for a laminate with strain-softening.

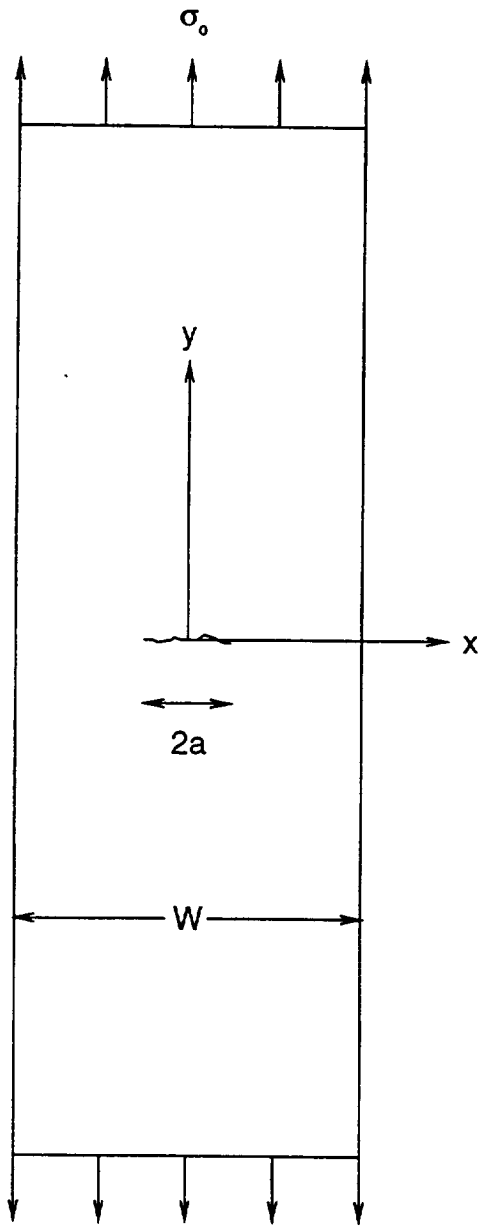

Fig. 2. Center-cracked tension specimen.

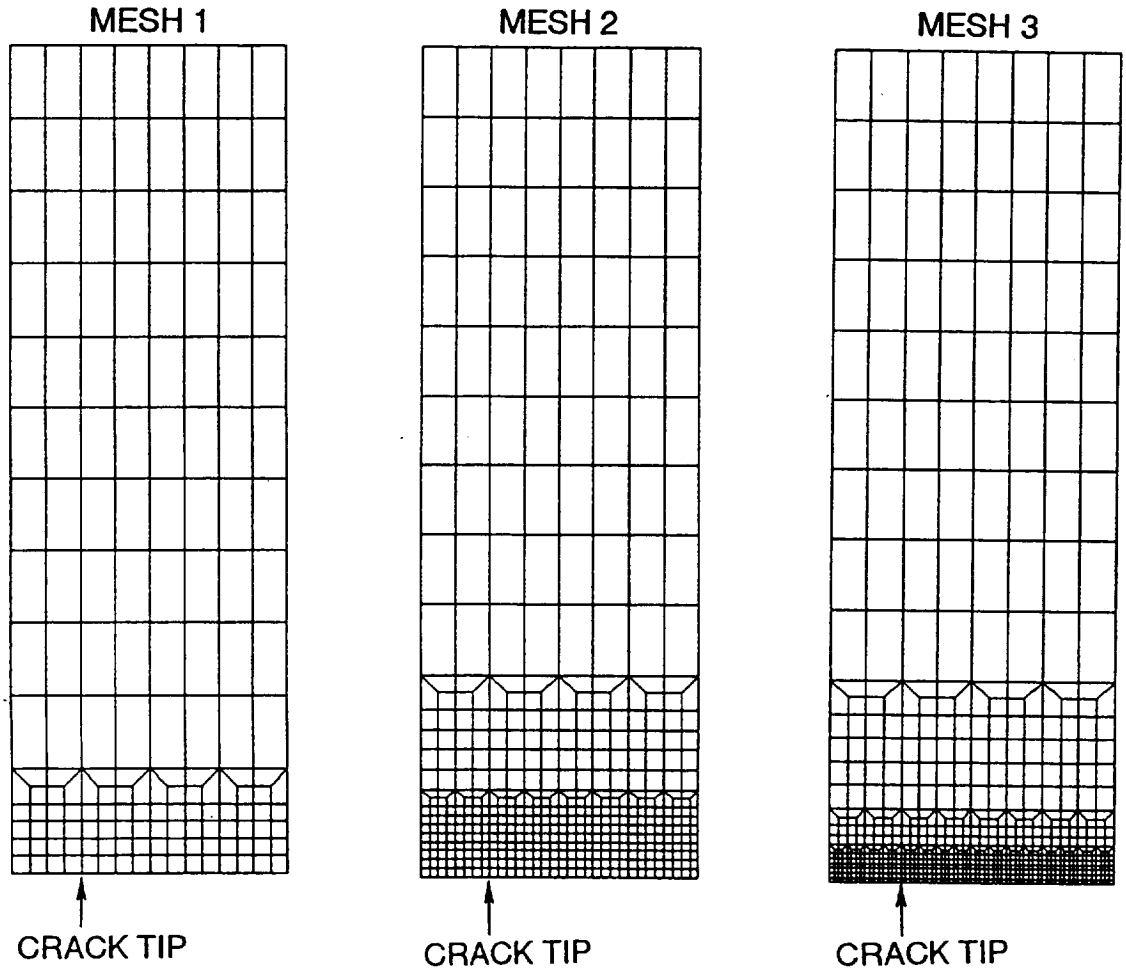

Fig. 3. Quarter-symmetry finite element meshes for a center-cracked tension specimen.

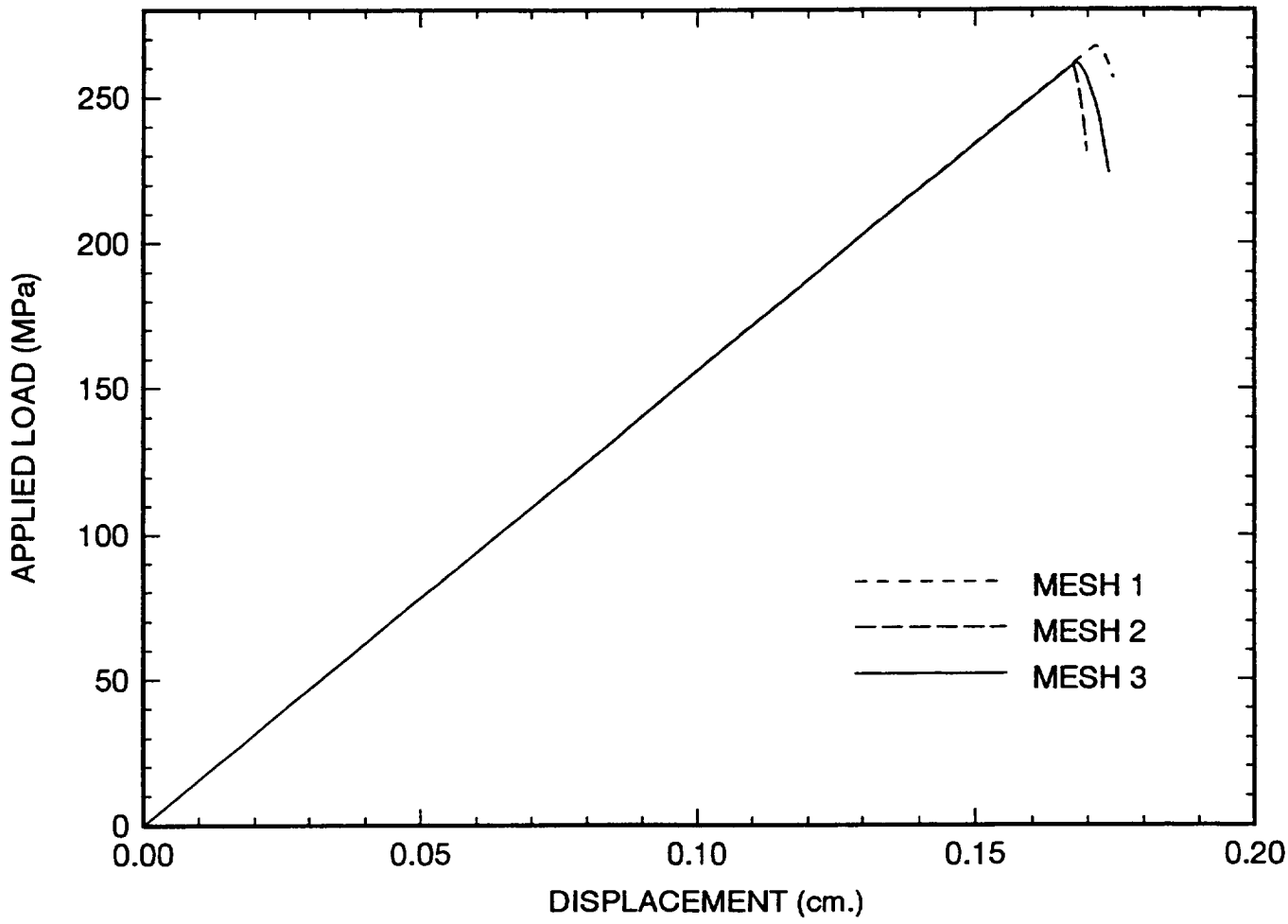

Fig. 4. Load-displacement curves for a center-cracked tension specimen modeled with three different finite element meshes.

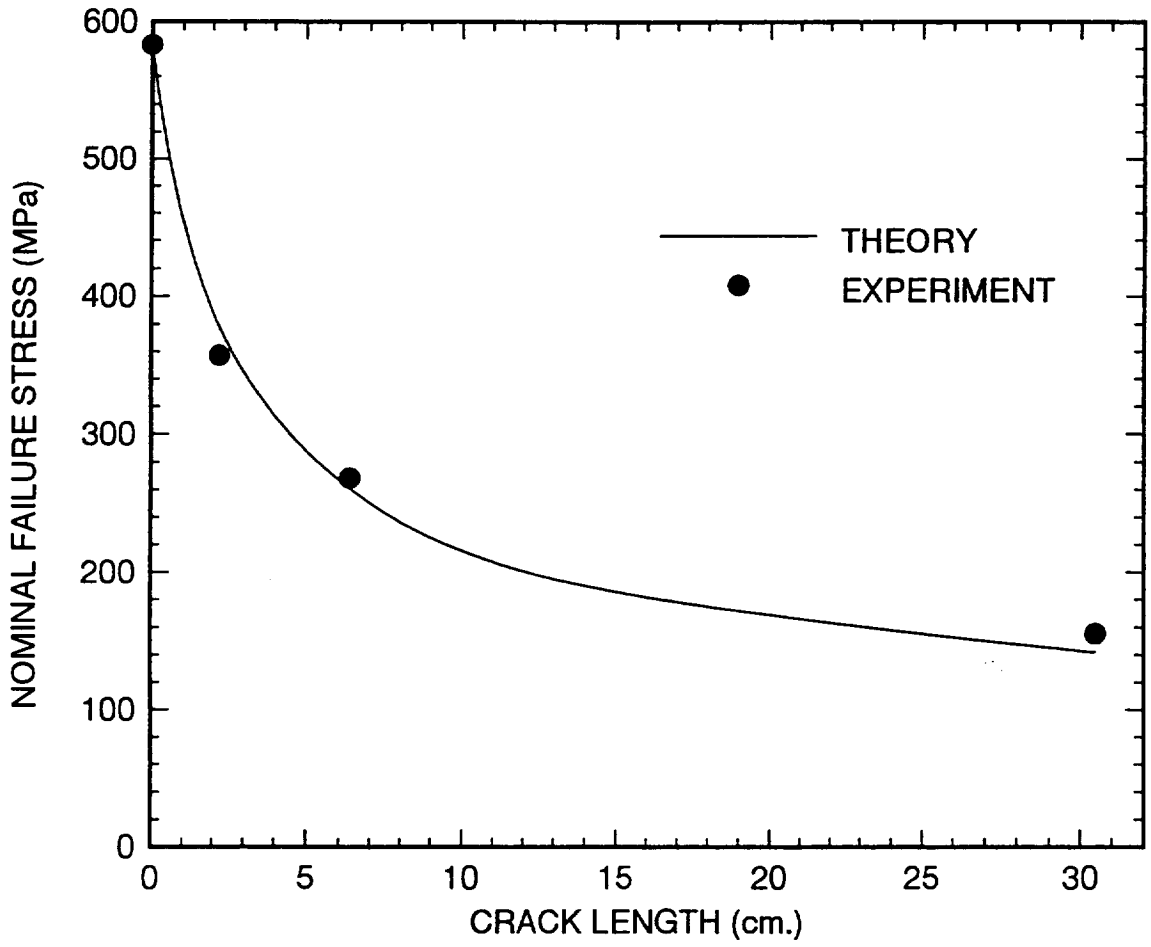

Fig. 5. Nominal failure stress versus crack length for a center-cracked tension specimen (13-ply laminate).

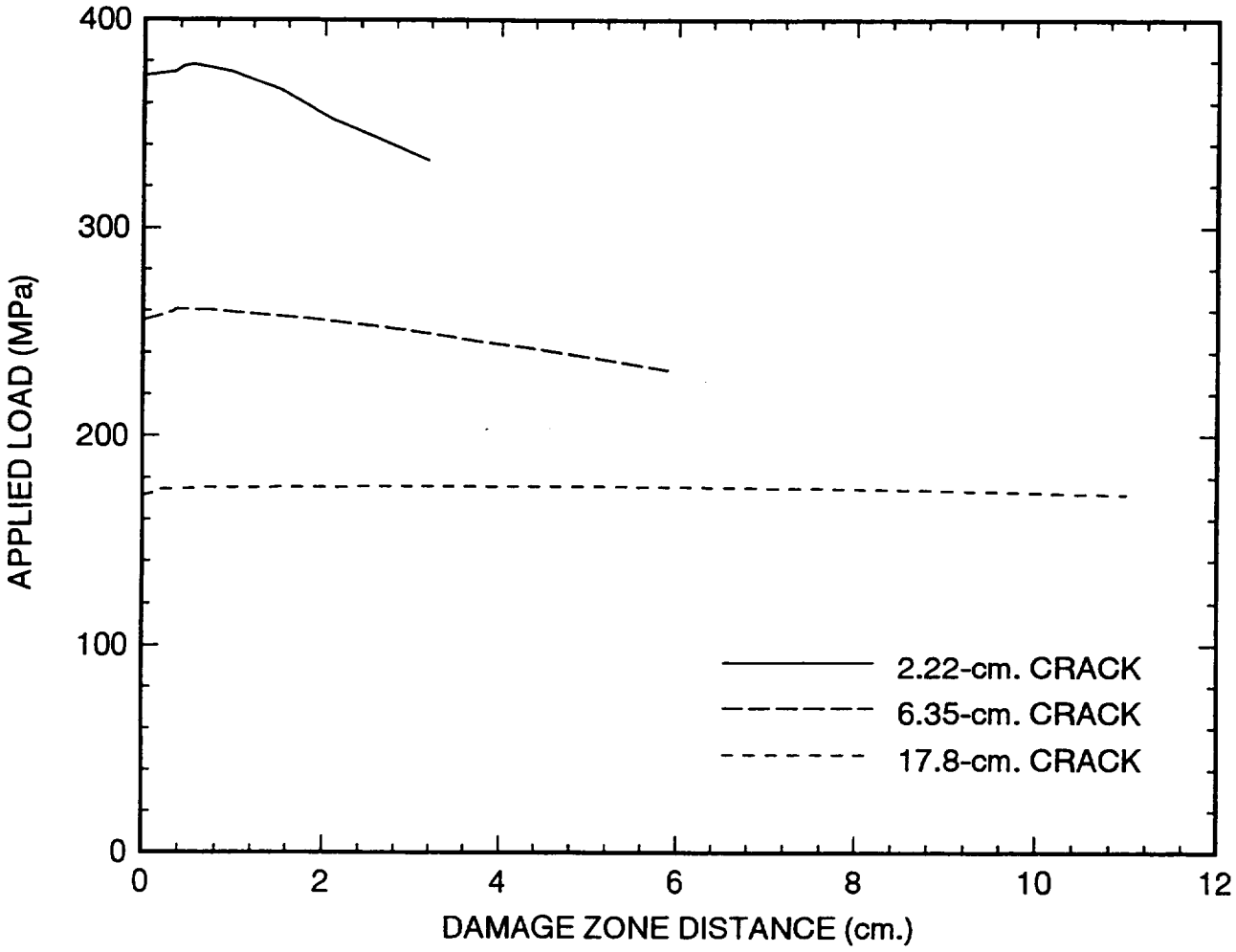

Fig. 6. Applied load versus damage zone distance for three different crack lengths (13-ply laminate).

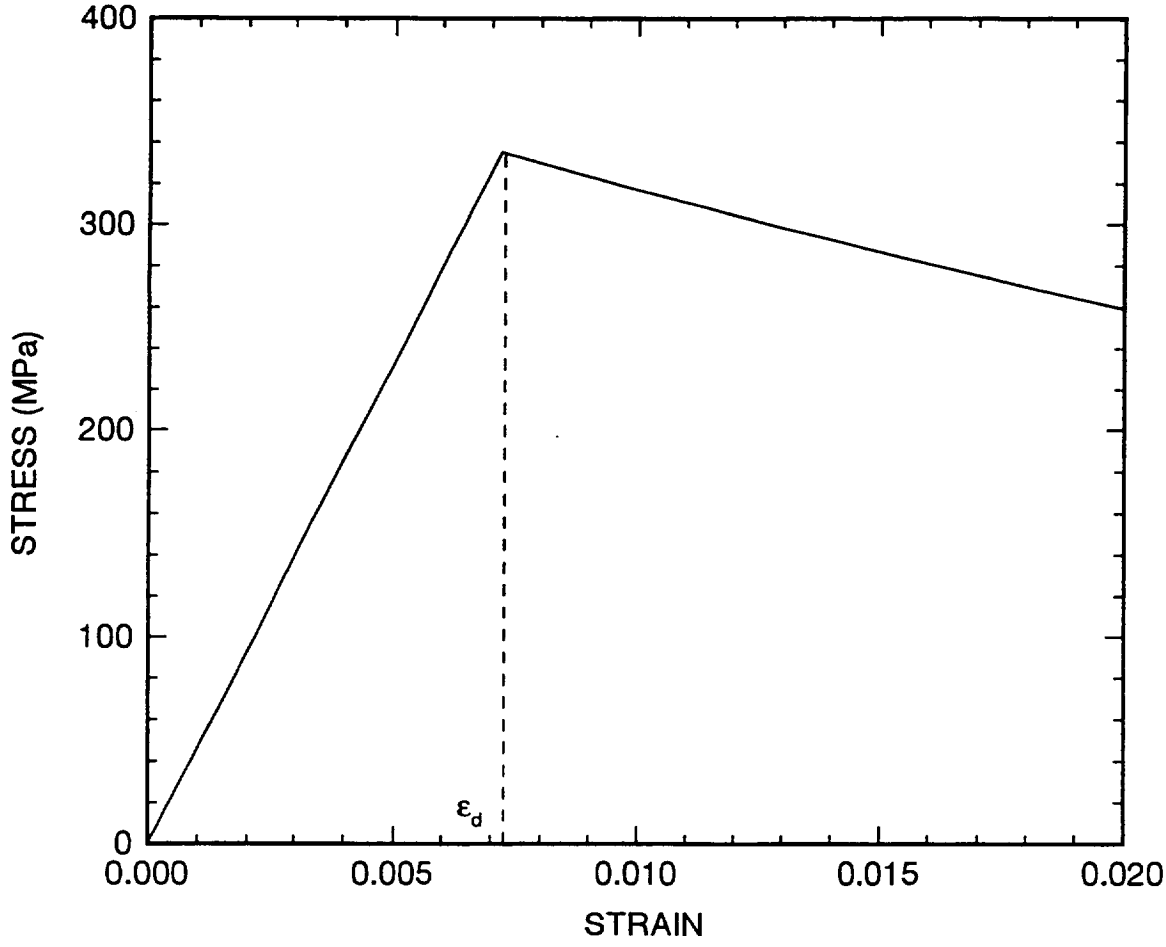

Fig. 7. Stress-strain curve for the 15-ply laminate.

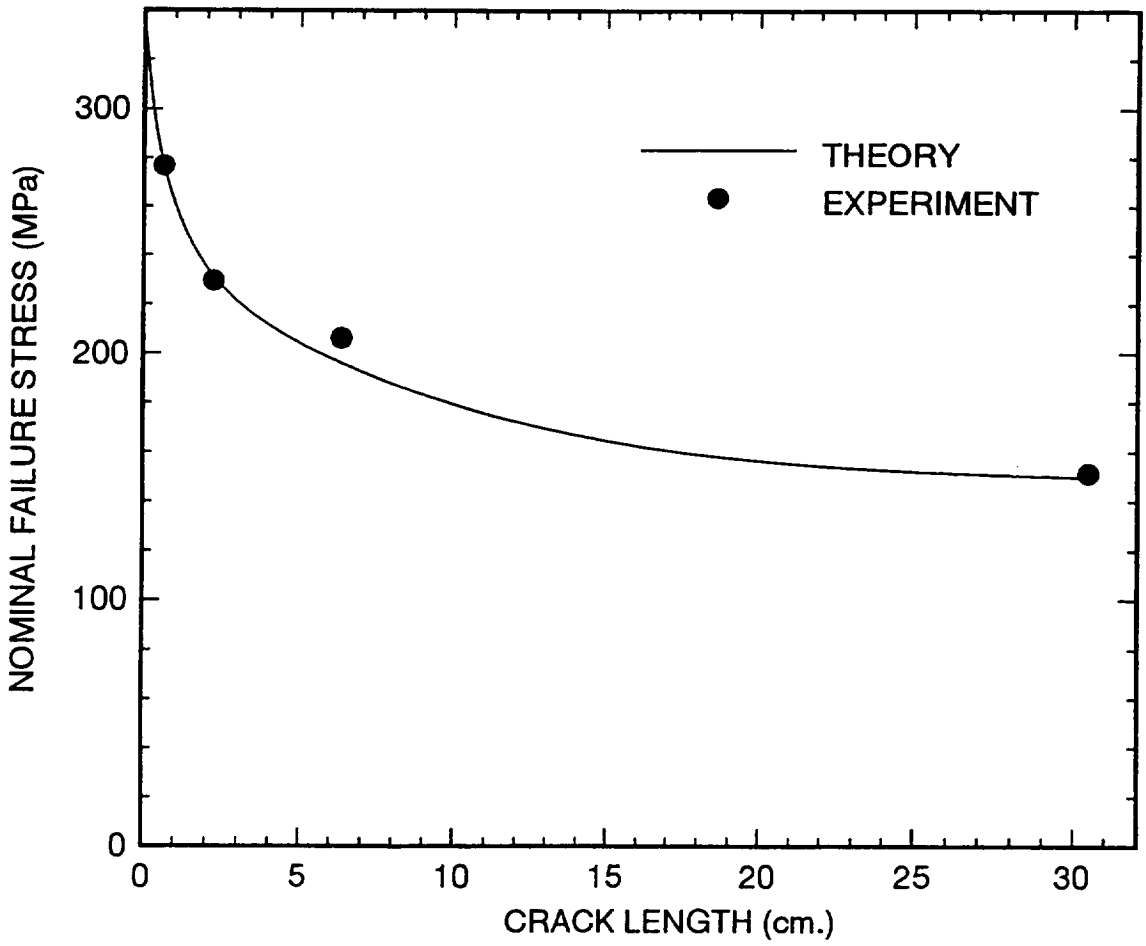

Fig. 8. Nominal failure stress versus crack length for a center-cracked tension specimen (15-ply laminate).

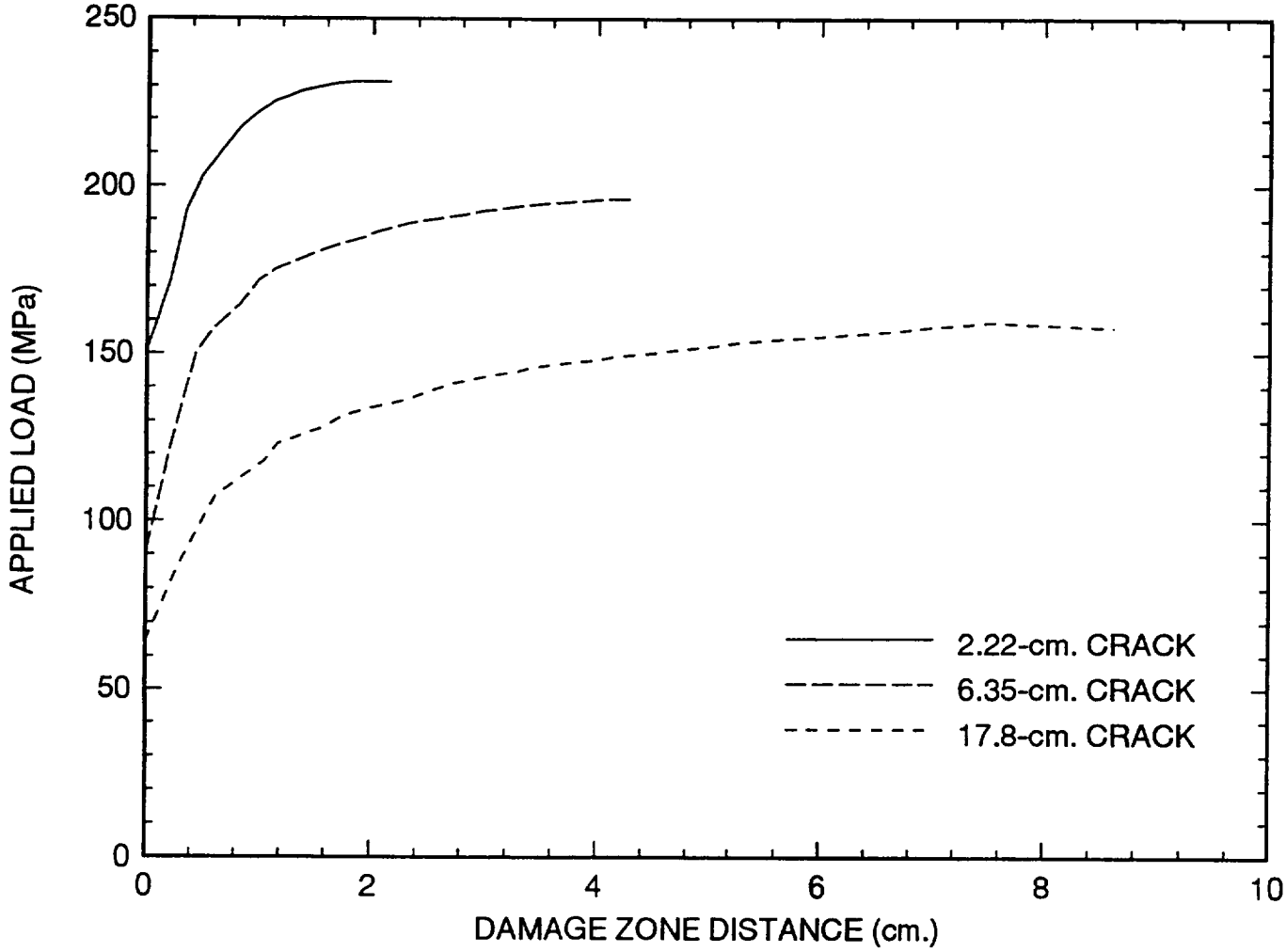

Fig. 9. Applied load versus damage zone distance for three different crack lengths (15-ply laminate).